

# **Brittle Fracture of Rock**

Evert Hoek

Chapter 4 in *Rock Mechanics in Engineering Practice*

Edited by K.G. Stagg and O.C. Zienkiewicz

London: J. Wiley, 99 to 124

1968

## **4.1 Introduction**

In chapters 1 and 2 the mechanical properties of rock materials have been discussed in some detail and it has been shown that most rocks exhibit patterns of behaviour which can be usefully employed by the practical engineer. Since most of the conclusions presented in chapters 1 and 2 are based upon empirical studies it is of interest to examine the basic mechanism of brittle failure of rock in order to gain some understanding of the underlying reasons for the behaviour patterns which are observed. Not only does such an examination satisfy the curiosity of the academically inclined but it also provides a basis for meaningful extrapolation from available experimental results.

A comprehensive review of the research effort which has been devoted to the study of the brittle failure of rock has recently been presented by Jaeger (1966). Rather than present yet another review on the theoretical aspects of this subject the author has chosen to present the known physical facts in a form which will be both meaningful and useful to the practical engineer. In order to achieve this end within the limited space available in this chapter, the dynamic aspects of rock fracture have been ignored and the discussion is limited to failure under quasi-static loading conditions such as those which can be expected to occur in rock structures.

## **4.2 Fracture initiation**

A rock material contains a large number of randomly oriented zones of potential failure in the form of grain boundaries. Let us assume that one such grain boundary, illustrated in figure 4.1, contains a number of open flaws and that, in accordance with the concept postulated by Griffith (1921, 1924), these flaws are approximately elliptical in shape. It can be shown that very high tensile stresses occur on the boundary of a suitably oriented elliptical opening, even under compressive stress conditions, and it is assumed that fracture initiates from the boundary of an open flaw when the tensile stress on this boundary exceeds the local tensile strength of the material.

In order to obtain an estimate of the stresses around the boundary of an open elliptical flaw it is necessary to make the following simplifying assumptions:

- a) The ellipse can be treated as a single opening in a semi-infinite elastic medium, i.e. adjacent flaws do not interact and local variations in material properties are ignored.
- b) The ellipse and the stress system which acts upon the material surrounding it can be treated two dimensionally, i.e. the influence of the three-dimensional shape of a flaw and of the stress  $\sigma_z$  in the crack plane can be ignored.

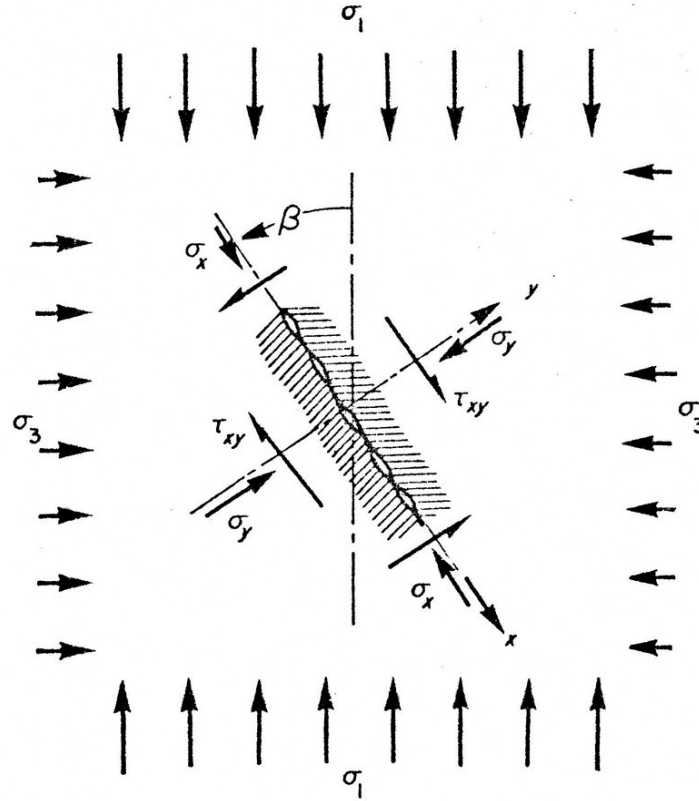


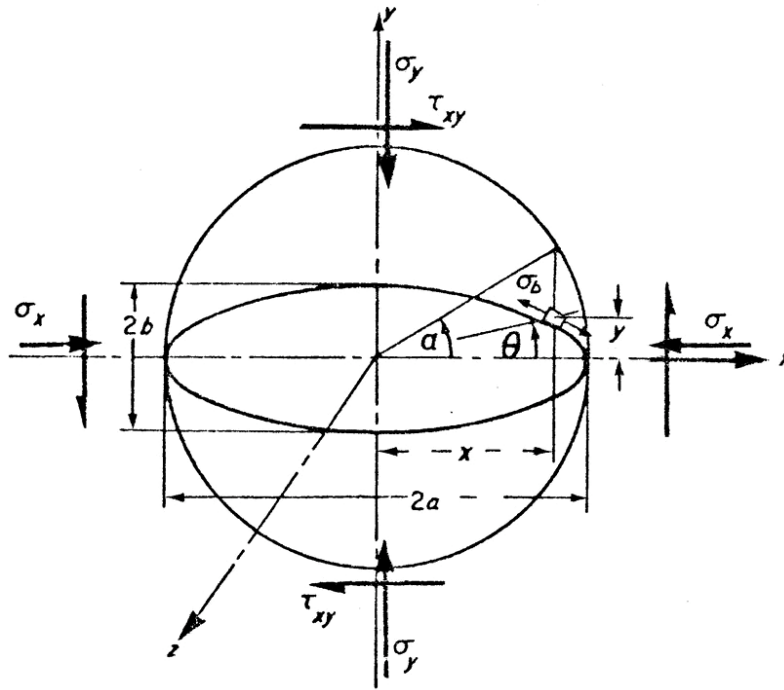
Figure 4.1 Stress system acting on a potential failure plane in rock.

Although these assumptions do introduce certain errors (Jaeger 1966), the magnitude of these errors is estimated to be less than  $\pm 10\%$  which is within the order of accuracy aimed at in this analysis.

The stress system acting upon the grain boundary under consideration is shown in Figure 4.1. The convention adopted in this analysis is such that compression is regarded as positive and that  $\sigma_1 > \sigma_2 > \sigma_3$  where  $\sigma_1, \sigma_2$  and  $\sigma_3$  are the three principal stresses acting on the rock body. The elliptical flaw is inclined at an angle  $\beta$  to the major stress direction, i.e. the direction of maximum compressive stress. The normal stress  $\sigma_y$  and the shear stress  $\tau_{xy}$  which act on the material surrounding the elliptical flaw are related to the maximum and minimum principal stresses  $\sigma_1$  and  $\sigma_3$  by the following equations:

$$2\sigma_y = (\sigma_1 + \sigma_3) - (\sigma_1 - \sigma_3) \cos 2\beta \quad (4.1)$$

$$2\tau_{xy} = (\sigma_1 - \sigma_3) \sin 2\beta \quad (4.2)$$



Equation of ellipse:

$$x = a \cdot \cos \alpha,$$

$$y = b \cdot \sin \alpha,$$

where  $\alpha$  is the eccentric angle;

$$\tan \theta = m \cdot \tan \alpha,$$

where  $m = b/a$ .

Figure 4.2 Stresses acting on the material surrounding a two-dimensional elliptical flaw.

The stress  $\sigma_x$  which acts parallel to the axis of the elliptical flaw and the intermediate principal stress  $\sigma_z$  which acts in the  $z$  direction will be shown to have a negligible influence upon the stresses near the tip of the flaw and can be ignored.

### *Brittle fracture of rock*

In the discussion which follows, the stress system will be discussed in terms of the normal and shear stresses  $\sigma_y$  and  $\tau_{xy}$  only. The interested reader can revert to the principal stresses  $\sigma_1$  and  $\sigma_3$  at any stage of the analysis by substitution of the relations given in equations (4.1) and (4.2).

The parameters which define the boundary of the elliptical flaw are given in Figure 4.2 and, of these, the most important are the ratio of the minor to the major axis of the ellipse  $b/a = m$  and the eccentric angle  $\alpha$  which defines the position of a point on the boundary of the ellipse. The tangential stress on the boundary of the ellipse  $\sigma_b$  is given by the following equation (Inglis 1913; Denkhaus 1964):

$$\sigma_b = \frac{\sigma_y \{m(m+2)\cos^2 \alpha - \sin^2 \alpha\} + \sigma_x \{(1+2m)\sin^2 \alpha - m^2 \cos^2 \alpha\} - \tau_{xy} \{2(1+m^2)\sin \alpha \cos \alpha\}}{m^2 \cos^2 \alpha + \sin^2 \alpha} \quad (4.3)$$

In a material such as rock it can be assumed that the elliptical flaws will have a very small axis ratio  $m$ , i.e. they will be very flat in shape. This means that the maximum tensile stress will occur near the tip of the elliptical flaw, i.e. when the eccentric angle  $\alpha$  is very small. When  $\alpha \rightarrow 0$ ,  $\sin \alpha \rightarrow \alpha$  and  $\cos \alpha \rightarrow 1$ . Substitution of these relations into equation (4.3) and neglecting terms of the second order and higher which appear in the numerator gives the following approximate expression for the boundary stress  $\sigma_b$  near the tip of the elliptical flaw:

$$\sigma_b = \frac{2(\sigma_y \cdot m - \tau_{xy} \cdot \alpha)}{m^2 + \alpha^2} \quad (4.4)$$

An important fact which emerges from this simplification is that the stress  $\sigma_x$ , which lies parallel to the major axis of the ellipse, has a negligible influence upon the boundary stress near the tip of the flaw. By analogy the influence of the intermediate principal stress  $\sigma_2 = \sigma_z$  can also be ignored.

The maximum tangential stress on the boundary of the elliptical flaw is given when

$$\frac{d\sigma_b}{d\alpha} = 0,$$

i.e. when

*Brittle fracture of rock*

$$(m^2 + \alpha^2)(-2\tau_{xy}) = 2(\sigma_y \cdot m - \tau_{xy} \cdot \alpha)2\alpha$$

Giving

$$\sigma_b = \frac{-\tau_{xy}}{\alpha}, \quad (4.5)$$

Or, rearranging in terms of  $1/\alpha$  :

$$\frac{1}{\alpha^2} + \frac{2\sigma_y}{m \cdot \tau_{xy}} \cdot 1 - \frac{1}{m^2} = 0 \quad (4.6)$$

Solving equation (4.6) for  $1/\alpha$  :

$$\frac{1}{\alpha} = \frac{1}{m \cdot \tau_{xy}} \left\{ \sigma_y \pm \sqrt{(\sigma_y^2 + \tau_{xy}^2)} \right\} \quad (4.7)$$

From equations (4.5) and (4.7)

$$\sigma_b \cdot m = -\sigma_y \pm \sqrt{(\sigma_y^2 + \tau_{xy}^2)} \quad (4.8)$$

The assumed criterion for fracture initiation is that a crack will propagate from the boundary of the elliptical flaw when the tangential stress  $\sigma_b$  reaches a limiting value equal to the tensile strength of the material at that point. Since it is not practical to measure either the local tensile strength of the material surrounding the flaw or the axis ratio  $m$ , it is convenient to express the term  $\sigma_b \cdot m$  in equation (4.8) in terms of a quantity which can be measured more readily. Such a quantity is the uniaxial tensile strength  $\sigma_t$  of the rock body which contains the flaw under consideration and this is obtained when  $\sigma_y = \sigma_t$  and  $\tau_{xy} = 0$  giving

$$\sigma_b \cdot m = -2\sigma_t \quad (4.9)$$

Substituting this relation into equation (4.8) and squaring both sides of the resulting equation gives

$$\tau_{xy}^2 = 4\sigma_t(\sigma_t - \sigma_y) \quad (4.10)$$

This equation, which is the equation of a parabola in the  $\tau_{xy} - \sigma_y$  plane, defines the

### Brittle fracture of rock

relation between the shear and normal stresses  $\tau_{xy}$  and  $\sigma_y$  at which fracture initiates on the boundary of an open elliptical flaw. Note that, in substituting a numerical value for the uniaxial tensile strength  $\sigma_t$ , it is necessary to include a negative sign in order to satisfy the sign convention adopted in this chapter. Hence a particular rock will have a uniaxial tensile strength of  $-2000 \text{ lb/in}^2$ .

### 4.3 Fracture propagation

If it is assumed that the inclination  $\beta$  of the elliptical flaw is such that the boundary stress  $\sigma_b$  is a maximum for any combination of the principal stresses  $\sigma_1$  and  $\sigma_3$  then equation (4.10) becomes the equation of an envelope to a number of Mohr circles, one of which is illustrated in Figure 4.3.

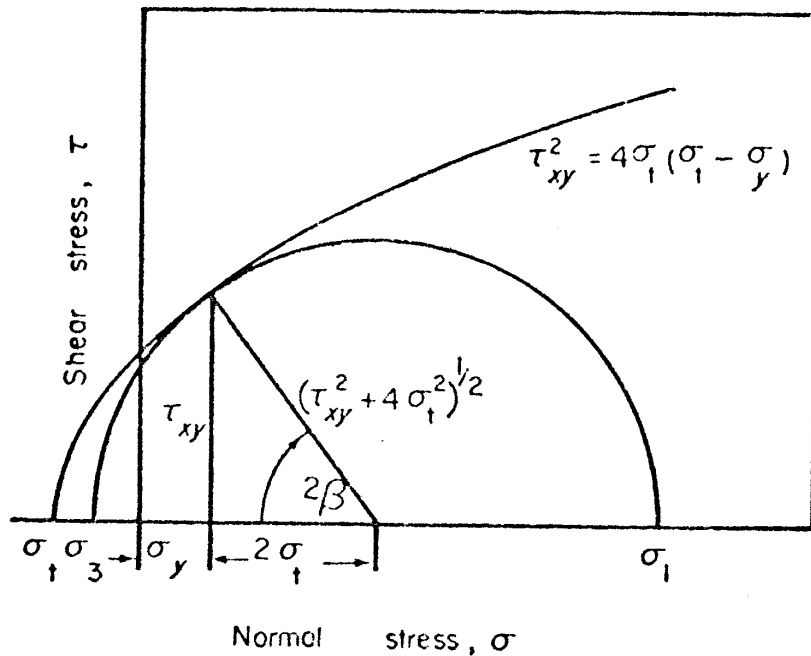


Figure 4.3. Relation between the normal and shear stresses required to initiate tensile fracture from an elliptical flaw.

From the geometry of this circle and from the slope of the normal to the envelope defined by equation (4.10) it follows that

$$\tan 2\beta = \frac{-d\sigma_y}{d\tau_{xy}} = \frac{\tau_{xy}}{2\sigma_t} \quad (4.11)$$

*Brittle fracture of rock*

From equations (4.5) and (4.9)

$$\sigma_b \cdot m = 2\sigma_t = \frac{-m \cdot \tau_{xy}}{\alpha},$$

hence

$$\alpha = \frac{-m \cdot \tau_{xy}}{2\sigma_t} = -m \cdot \tan 2\beta, \quad (4.12)$$

which defines the relations between the position of the maximum tensile stress on the boundary of the elliptical flaw ( $\alpha$ ) and the inclination of this flaw ( $\beta$ ) to the direction of the minimum principal stress  $\sigma_3$ .

Since fracture is assumed to occur when the tangential stress on the boundary of the flaw exceeds the local tensile strength of the material, it can be assumed that the crack will propagate in a direction which is normal to the boundary of the ellipse. The normal to the ellipse defined by the equation given in Figure 4.2 is defined by

$$\tan \gamma = \frac{-dx}{dy},$$

where

$$\left. \begin{aligned} dx &= -a \cdot \sin \alpha \cdot d\alpha \\ dy &= ma \cdot \cos \alpha \cdot d\alpha \end{aligned} \right\} \quad (4.13)$$

Hence

$$\tan \gamma = \frac{\tan \alpha}{m} \quad (4.14)$$

But, since  $\alpha$  is small,  $\tan \alpha \rightarrow \alpha$ , hence

$$\tan \gamma = \frac{\alpha}{m} = -\tan 2\beta \quad (4.15)$$

or

$$\gamma = -2\beta \text{ or } (\pi - 2\beta) \quad (4.16)$$

This relation is illustrated in Figure 4.4. From equation (4.11) it can be seen that as soon as  $\tau_{xy} > 0$ ,  $\beta > 0$ , therefore  $\gamma > 0$  and hence the crack which initiates on the boundary of the flaw will tend to propagate out of the plane of the flaw. This is a very important result and it is interesting to investigate the propagation of this crack in greater detail.

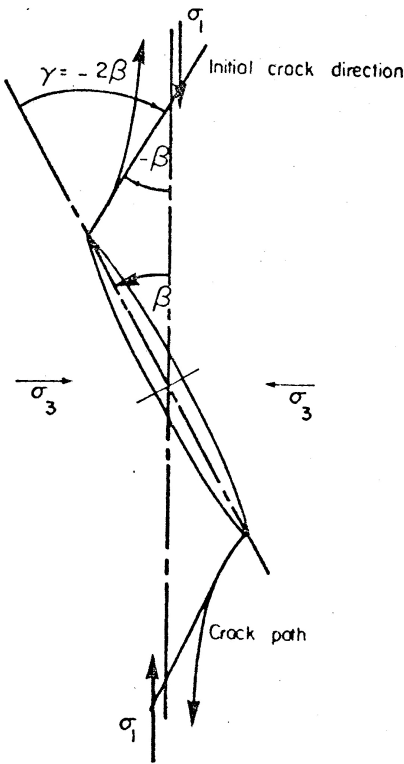


Figure 4.4 Direction of crack propagation from the tip of an elliptical flaw under compressive stress conditions.

#### 4.3.1 Fracture propagation when $\tau_{xy} = 0$

From equations (4.11) and (4.16), when  $\tau_{xy} = 0$ ,  $\beta = 0$  and  $\lambda = 0$ . In other words, under conditions of uniaxial tensile stress to which the crack is perpendicular, a crack is initiated at the tip ( $\alpha = 0$ ) of the elliptical flaw and it will propagate in the plane of the initial flaw.

Substituting  $\tau_{xy} = 0$  and  $\alpha = 0$  in equation (4.4) gives

$$\sigma_b = \frac{2\sigma_y}{m} = \frac{2\sigma_3}{m} \quad (4.17)$$

If it assumed that the radius of curvature of the propagating crack is of the same order of magnitude as the radius of curvature of the original elliptical flaw, then propagation of this crack has the same effect as decreasing the axis ratio  $m$  of the original flaw. From

### *Brittle fracture of rock*

equation (4.17) it will be seen that this results in an increase in the boundary stress  $\sigma_b$  and hence the crack will continue to propagate, even if the applied stresses are decreased.

Under these conditions the propagation of this crack results in tensile rupture<sup>1</sup> of the specimen. An important conclusion which can be drawn from this discussion is that tensile rupture will occur in a plane defined by  $\beta=0$ , i.e. in a plane which is perpendicular to the direction of the applied tensile stress  $\sigma_3$ .

#### **4.3.2 Fracture propagation when $\tau_{xy} > 0$**

As already discussed, when  $\tau_{xy} > 0$ , the crack which initiates on the boundary of the elliptical flaw propagates out of the plane of this flaw. It has been demonstrated experimentally (Brace & Bombolakis 1963; Hoek & Bieniawski 1965) and theoretically (Paul & Gangal 1966; Bray, personal communication) that this propagating crack will follow a curved path as indicated in Figure 4.4. This crack path tends to align itself along the direction of the major principal stress  $\sigma_1$  which, in effect, gives rise to a situation in which the equivalent elliptical flaw is inclined at  $\beta=0$  and the stress at the tip of the propagating crack can be approximated from equation (4.17).

When  $\sigma_3 > 0$ , i.e. when  $\sigma_3$  is compressive, an entirely different situation occurs in that the stress at the tip of the propagating crack becomes compressive when the crack is aligned in the direction of the major principal stress  $\sigma_1$ . Under these conditions propagation of the crack will cease and the new flaw so created will be stable under the existing conditions of applied stress.

The length of the crack which propagates from an open elliptical flaw for a given combination of applied stresses has been determined experimentally by Hoek and Bieniawski (1965) and the results of these experiments are plotted in Figure 4.5.

The important conclusion to be drawn from these results is that a single open elliptical flaw cannot cause rupture of a rock specimen under conditions in which that applied stresses ( $\sigma_1$  and  $\sigma_3$ ) are both compressive.

---

<sup>1</sup> In this discussion the disintegration of the specimen into two or more separate pieces will be termed *rupture*.

#### **4.4 Rock fracture in compression**

When the principal stresses  $\sigma_1$  and  $\sigma_3$  applied to a rock body containing an open elliptical flaw are both compressive, the crack which is initiated on the boundary of this flaw will only propagate a short distance before it stops and becomes stable (Figure 4.5). In considering the problem of rupture under compressive stress, it is necessary to determine the conditions necessary to propagate the stable crack described above or the conditions necessary to initiate some new failure mode.

Experimental evidence obtained by Hoek and Bieniawski (1965) suggests that propagation of the stable cracks which were initiated from open flaws occurs when the shear resistance of the zone containing these flaws is overcome and shear movement occurs as suggested in Figure 4.6.

The condition for the onset of shear movement may be expressed by the following equation:

$$\tau_{xy} = \tau_o + \mu\sigma_y \quad (4.18)$$

where  $\tau_o$  is the intrinsic shear resistance of the material, i.e. the shear resistance when the normal stress  $\sigma_y = 0$  and which is due to interlocking of asperities and to cohesive forces. The coefficient of internal friction  $\mu$  is the ratio between the shear stress  $\tau_{xy}$  required to sustain movement, once the intrinsic shear resistance  $\tau_o$  has been overcome, and the normal stress  $\sigma_y$ .

The criterion expressed by equation (4.18) is familiar to most engineers and is most commonly associated with the names of Navier, Coulomb and Mohr (see Jaeger's 1966 review for historical details).

Since the condition expressed by equation (4.18) is that required to initiate shear movement, it does not follow automatically that this equation defines the conditions for rupture of the specimen. Consequently it is necessary to consider the events which follow initiation of the shear movement in order to establish whether rupture of the specimen will occur.

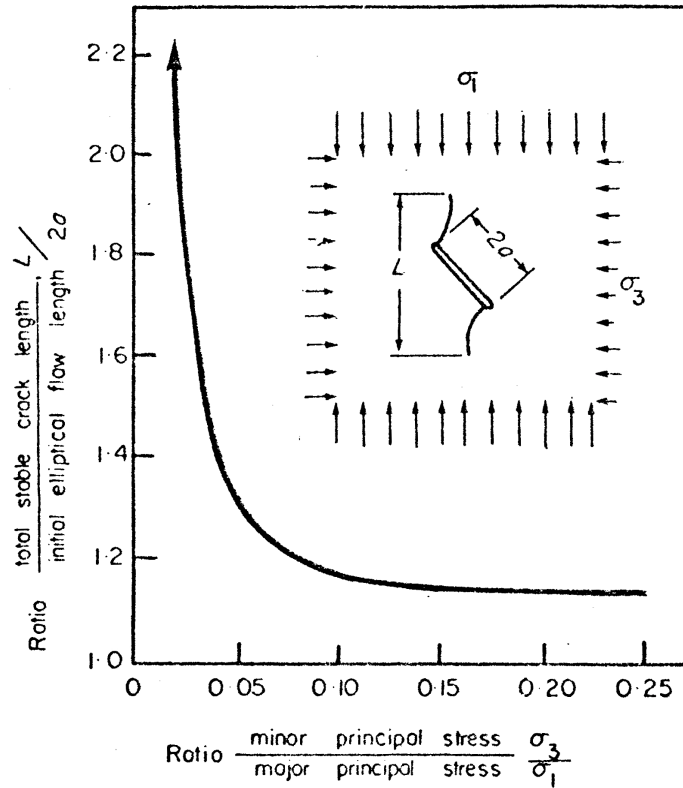


Figure 4.5 Length of stable crack propagated from an elliptical flaw under compressive stress conditions Hoek & Bieniawski 1965

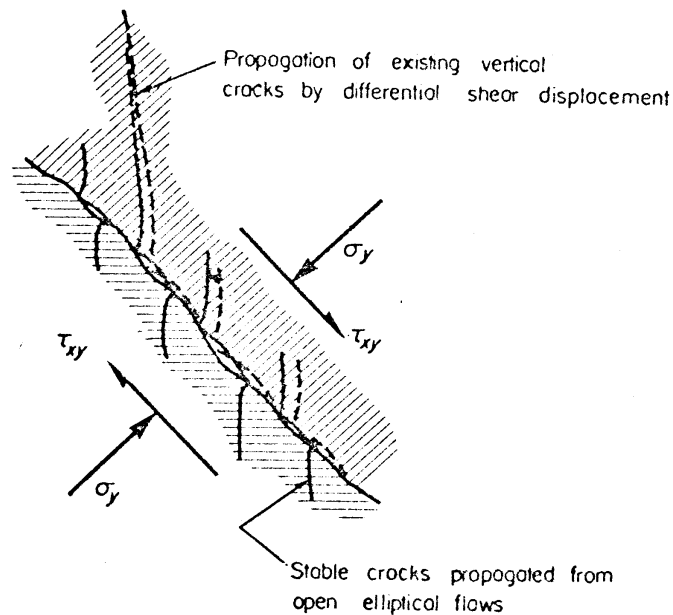


Figure 4.6 Mechanism of fracture propagation caused by displacement on a shear plane

### *Brittle fracture of rock*

In applying the Navier-Coulomb criterion, equation (4.18), to a rock failure problem it is usual to assume that rupture of the specimen takes place as a result of shear movement along a plane inclined at an angle  $\beta$  to the minor principal stress direction as suggested in Figure 4.7(a). The relation between the angle  $\beta$  and the coefficient of internal friction  $\mu$  can be found by considering the slope of the Mohr envelope as was done earlier in this paper in the case of the Griffith criterion (Figure 4.3):

$$\tan 2\beta = \frac{-d\sigma_y}{d\tau_{xy}} = \frac{-1}{\mu} \quad (4.19)$$

While it is accepted that simultaneous movement on the shear plane is a valid failure mode it is suggested that interlocking of asperities on this plane can also give rise to differential shear movement which results in the propagation of existing vertical cracks, as suggested in Figure 4.6. This would result in the vertical tensile type of rupture illustrated in Figure 4.7(b).

A third possibility is that rupture can occur as a result of some combination of the two modes discussed above, giving a rupture surface which is intermediate between the direction of the major principal stress  $\sigma_1$  and the direction of the shear plane which is inclined at an angle  $\beta$  to the major principal stress direction.

A final possibility is that the propagation of either of the above modes could be inhibited by changes in either the stress field or the material properties in the crack path, resulting in a stable crack configuration such as that illustrated in Figure 4.7(c). Propagation of this stable crack system would require a further increase in the applied compressive stress  $\sigma_1$ .

It will be evident to the reader, from the discussion given above, that the final appearance of a rock specimen which has been tested to rupture under compressive stress conditions will depend upon the size of the specimen and upon the degree of restraint imposed by the testing machine platens. The influence of laboratory test procedures upon the results of rupture tests on rock specimens will be discussed in a later section of this chapter in which the application of such results to practical rock mechanics problems is discussed.

Factors which influence the material 'constants'  $\sigma_f$ ,  $\tau_o$  and  $\mu$  and the effect of changes in

## *Brittle fracture of rock*

these constants upon the behaviour of the material will also be discussed in a later section of this chapter.

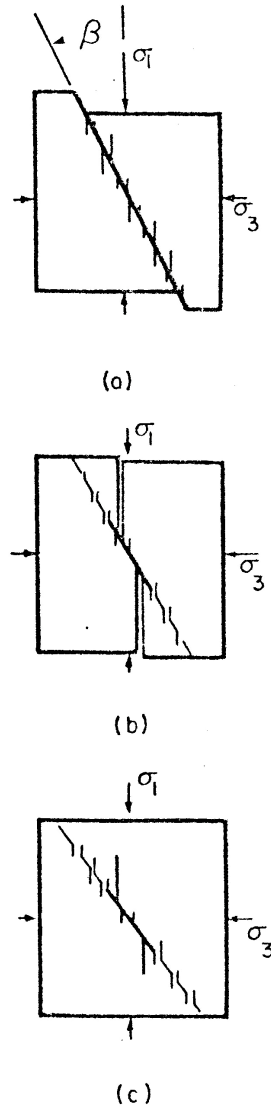


Figure 4.7 Suggested rupture modes under compressive stress conditions, (a) Shear failure; (b) Tensile failure; (c) Stable crack configuration.

### **4.5 A rupture criterion for brittle rock**

In order to obtain the simplest possible rupture criterion for a brittle rock, consider the behaviour of a specimen which contains a large number of randomly oriented flaws of similar size and shape, for example, a carefully selected sample of a homogeneous fine-

*Brittle fracture of rock*

grained rock, such as Witwatersrand quartzite (Hoek 1966). Such a material will exhibit no significant anisotropy in its strength behaviour and will have a uniaxial compressive strength of approximately ten times its uniaxial tensile strength.

The rupture criterion for such a material can be expected to be a logical extension of the fracture initiation criteria already discussed and the complete rupture criterion is illustrated in Figure 4.8.

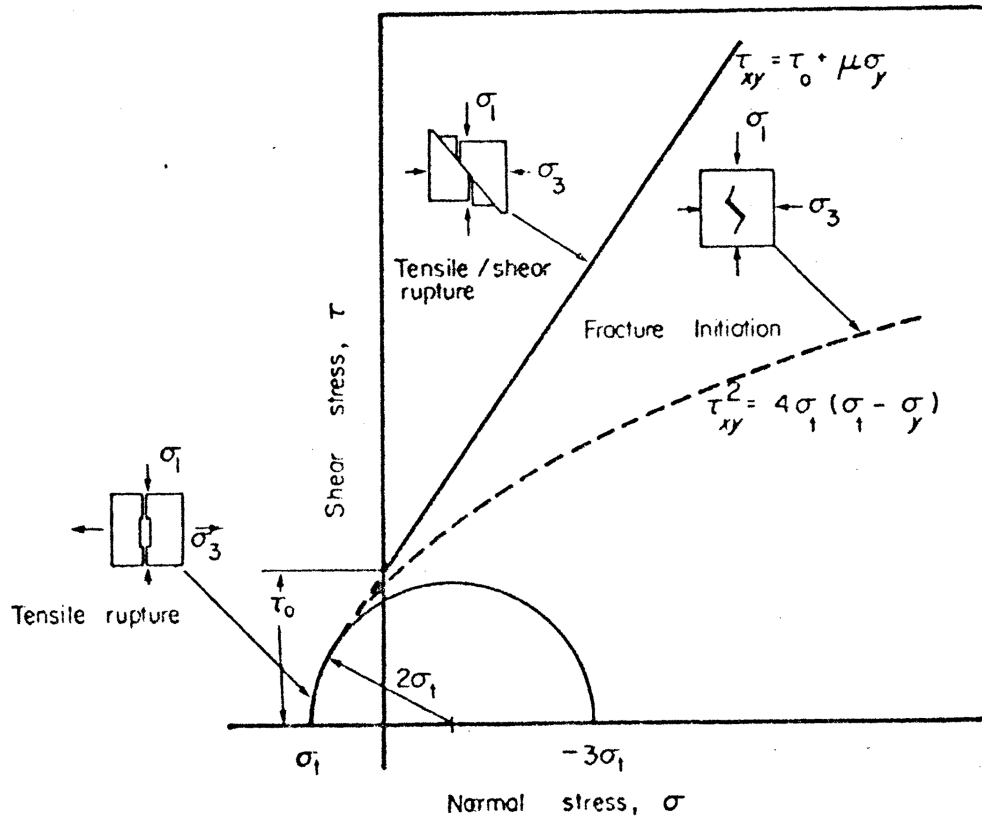


Figure 4.8 A rupture criterion for brittle rock.

In deriving this rupture criterion the following factors were taken into consideration.

(a) The simplest type of tensile rupture occurs when the minor principal stress equals the uniaxial tensile strength of the material, i.e.  $\sigma_3 = \sigma_t$ . This rupture is caused by the propagation of a crack which initiates at the tip ( $\alpha = 0$ ) of the flaw which is perpendicular to the minor principal stress direction ( $\beta = 0$ ). The conditions under which this type of rupture occurs can be deduced from figure 4.3, from which it can be seen that the radius of curvature of the Mohr envelope at the point of its intersection with the

### *Brittle fracture of rock*

normal stress axis ( $\tau_{xy} = 0$ ) is equal to  $2\sigma_t$ . Consequently, all Mohr stress circles which fall within this circle of radius  $2\sigma_t$  (see Figure 4.8) can only touch the rupture envelope at one point which is defined by  $\tau_{xy} = 0$  and  $\sigma_3 = \sigma_t$ . This implies that pure tensile rupture occurs when  $\sigma_1 \leq -3\sigma_3$ .

b) Rupture of a rock specimen, when the normal stress acting on the potential shear surface is compressive ( $\sigma_y > 0$ ), is assumed to occur when the shear resistance of this plane is overcome, i.e. when equation (4.18) is satisfied. Shear movement on this plane can induce shear and/or tensile rupture of the specimen as suggested in Figure 4.7.

c) The transition between the conditions which govern pure tensile rupture and the conditions under which rupture is induced as a result of shear displacement cannot be derived directly from the fracture initiation criteria already discussed in this chapter. This difficulty is caused by the fact that the crack which initiates on the boundary of a flaw subjected to a finite shear stress will tend to propagate out of the plane of the flaw (see Figure 4.4). Although this crack will tend to align itself along the major principal stress direction it is not possible to calculate the magnitude of the minor principal stress  $\sigma_3$  which is required to cause rupture of the specimen. In order to overcome this difficulty it is proposed, on purely phenomenological grounds, that this transition should take the form suggested by the heavy dashed line in Figure 4.8, i.e. it is assumed that the straight-line rupture criterion which defines shear-induced rupture is tangential to the parabolic Mohr envelope which defines fracture initiation from open elliptical flaws.

From the geometry of the rupture diagram presented in Figure 4.8, it is possible to estimate the relation between the intrinsic shear strength  $\tau_o$  and the uniaxial tensile strength  $\sigma_t$ :

$$\tau_o = -\sigma_t \left( \frac{1}{\mu} + \mu \right) \quad (4.20)$$

The practical significance of this relation is that it enables an estimate of the maximum uniaxial tensile strength of a particular material to be obtained from the value of the intercept  $\tau_o$  of a Mohr rupture envelope fitted to a number of triaxial compression or shear test results.

Practical experience (Hoek 1966) confirms that the rupture criterion proposed in Figure 4.8 provides an adequate basis for predicting the stresses required to cause rupture of a

brittle rock material under the conditions normally encountered in mining or civil engineering rock mechanics problems<sup>2</sup>. However, from the discussion on the direction of fracture propagation (Figure 4.7), it is evident that no reliable estimate of the angle of rupture of a rock specimen can be made from the Mohr rupture diagram presented in Figure 4.8. In other words, the angle  $2\beta$  subtended by the normal to the rupture envelope (see Figure 4.3) defines the orientation of the flaw from which fracture initiates or upon which shear displacement occurs but it gives no information on the subsequent path which the fracture will follow. The author believes that the angle of rupture of an element of rock is critically dependent upon the restraints imposed upon it by the testing machine platens, in the case of a laboratory test, or by the surrounding material in the case of a rock structure. A great deal of careful thought and experimentation has still to be devoted to this problem in order to clarify the current confusion which exists in relation to the angle of rupture of rock materials.

#### **4.6 Factors which influence the rupture behaviour of rock**

The 'ideal' brittle material upon which the derivation of the fracture initiation and rupture criteria presented above is based cannot be considered representative of the material which would be found in a rock structure, such as a dam foundation or the rock surrounding a mine excavation. Nor can the conditions to which a carefully selected laboratory test specimen is subjected be regarded as representative of the wide variety of conditions which are likely to be encountered in the field.

Obviously, a theoretical rupture criterion which accounts for all possible deviations from the 'ideal' would be far too complex to have any practical value. On the other hand, the 'ideal' would be far too complex to have any practical value if some estimate can be made of the extent to which the rock behaviour is likely to be influenced by deviation from the idealized assumptions.

---

<sup>2</sup> Deviations from the linear Mohr envelope defined by equation (4.18) are discussed in a later section of this chapter.

#### 4.6.1 Influence of moisture on the strength of rock

The presence of moisture in a rock body can influence the rupture behaviour of the rock in two important ways:

a) The moisture can reduce the strength of the rock by chemical or physical alternation of its inherent properties. This strength reduction can be very important; for example, the results obtained by Colback and Wiid (Colback & Wiid 1965) for tests on a quartzitic shale (Figure 4.9) show that the strength of specimens which had been dried over calcium chloride for several weeks. This finding emphasizes the need to simulate field conditions as closely as possible in the laboratory and, if in doubt, to assume the worst conditions and to test the specimens in a saturated state.

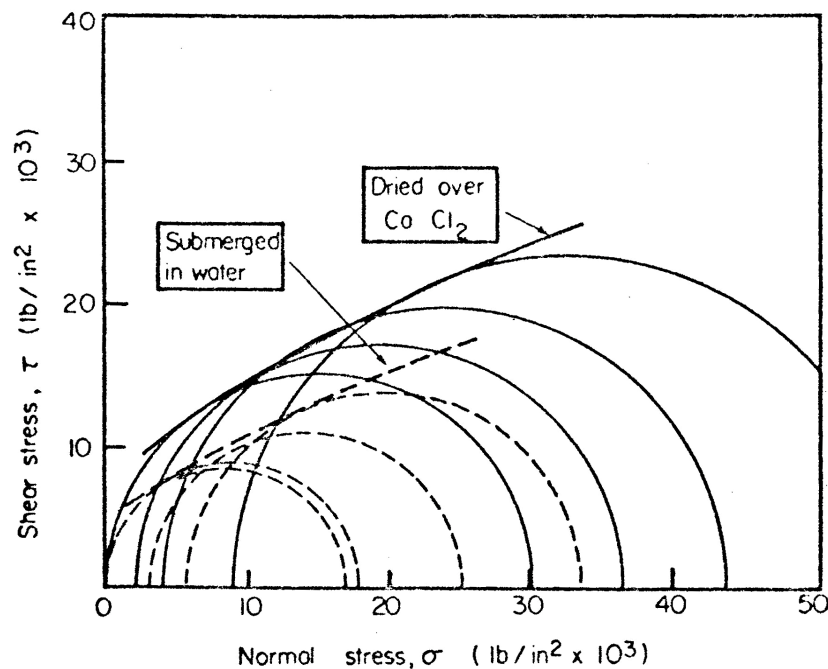


Figure 4.9. Mohr rupture envelopes showing the effect of moisture on the compressive strength of quartzite shale (Colback & Wiid 1965)

(b) If the moisture is present under pressure, the strength of rock is further reduced. Numerous experimental observations (e.g. Murreli 1966 and Byerlee in press) have

### *Brittle fracture of rock*

confirmed the theoretical prediction that the influence of pore pressure can be allowed for in the rupture criteria discussed in this chapter by replacing the normal stress  $\sigma_y$  by an effective stress  $(\sigma_y - p)$ . Noting that a compressive stress of magnitude  $p$  balances the internal pore pressure, it is clear that only the excess  $\sigma_y - p$  can be effective in developing tensions. Consequently, equation (4.10) becomes

$$\tau_{xy}^2 = 4\sigma_t \{ \sigma_t - (\sigma_y - p) \} \quad (4.21)$$

while equation (4.18) becomes

$$\tau_{xy} = \tau_o + \mu (\sigma_y - p) \quad (4.22)$$

It is important to note that in any testing involving a study of the influence of moisture or of pore-pressure effects, the rate of loading of the specimen is a critical factor. The discussion presented above is based upon static stress conditions and unless the rate of loading is low enough to permit the pore pressure to distribute itself uniformly throughout the volume of the specimen or, in the case of a drained test, to prevent the build up of dynamic pore pressures, the conclusions presented above will not be valid<sup>3</sup>.

#### 4.6.2 Influence of the normal stress upon the frictional behaviour of rock

The envelope fitted to a set of Mohr circles obtained from low pressure triaxial compression tests on brittle rocks is usually adequately represented by a straight line as suggested by equation (4.18) (Wuerker 1959). Since many civil and mining engineering applications involve low confining pressures (up to say one-half the uniaxial compressive strength of the rock), the assumption that the coefficient of friction  $\mu$  is a constant is sufficiently accurate for these applications.

However, in the case of problems involving high confining pressures such as those which may be encountered in deep-level mining or in problems of interest to the geologist, this

---

<sup>3</sup> Professor W. F. Brace of the Massachusetts Institute of Technology, in a personal communication to the author, gives the critical strain rate for the loading of a small specimen (approximately 0.5 inch diameter x 1.5 inches long) of Westerly granite as approximately  $10^{-7}$  in/in/s.

assumption can be seriously in error. The assumption that the coefficient of friction is a constant can also be misleading in the case of 'soft' rocks, such as shales and siltstones, which exhibit non-linear rupture envelopes, even at very low confining pressures.

Experimental evidence obtained by Murrell (1966), Hobbs (1966), Patton (1966) and Byerlee (in press) suggests that the coefficient of internal friction  $\mu$  in equation (4.18) is not a constant but depends upon the magnitude of the normal compressive stress  $\sigma_y$ . The reason for this breakdown of Amonton's law of friction is associated with the interlocking of the asperities on the shear plane (see Figure 4.6). This interlocking depends upon the intimacy of the contact of the asperities which, in turn, depends upon the magnitude of the normal stress  $\sigma_y$ .

Although a number of theoretical models of this interlocking behaviour have been considered (Murrell 1966; Hobbs 1966; Byerlee in press), the problem has not been adequately solved and, in the author's opinion, a considerable amount of theoretical work is still necessary. However, in the absence of a rigorous theoretical solution, a useful empirical solution can be obtained by assuming that the rupture behaviour of a brittle rock can be characterized by the following equation:

$$\tau_{\max} = \tau_{\max o} + A\sigma_m^b \quad (4.23)$$

where  $\tau_{\max} = \frac{1}{2}(\sigma_1 - \sigma_3)$  is the maximum shear stress,

$\sigma_m = \frac{1}{2}(\sigma_1 + \sigma_3)$  is the mean normal stress

and  $\tau_{\max o}$  is the intercept of the  $\tau_{\max}$  versus  $\sigma_m$  plot when  $\sigma_m = 0$ .

The reasons for the choice of the *maximum* shear stress  $\tau_{\max}$  and the *mean* normal stress  $\sigma_m$  in place of the shear and normal stresses  $\tau_{xy}$  and  $\sigma_y$  as suggested by (Murrell 1966) and (Hobbs 1966) are important and are worthy of some consideration.

In analysing the results of conventional triaxial compression tests, we are faced with the problem of determining the values of the shear and normal stresses  $\tau_{xy}$  and  $\sigma_y$  from the experimentally determined values of the applied axial and lateral stresses  $\sigma_1$  and  $\sigma_3$  ( $= \sigma_2$ ). If the inclination  $\beta$  of the plane upon which the shear and normal stresses act is

known, their values can be calculated from equations (4.1) and (4.2). However, as discussed earlier in this chapter, available evidence suggests that the fracture path is a complex one which may have no direct relation to the shear and normal stresses which were responsible for its initiation and propagation (see Figure 4.7b). In addition, current triaxial testing techniques are such that the fracture path is almost certainly influenced by platen effects and by the non-uniformity of the stress distribution in the specimen at the final stages of rupture. Consequently, any attempt to determine the inclination  $\beta$  of the rupture surface from the configuration of a ruptured triaxial specimen must be treated with suspicion.

In order to overcome these difficulties, the author suggests the use of the maximum shear stress and the mean normal stress which can be calculated directly from the axial stress  $\sigma_1$  and confining pressure  $\sigma_3$  values obtained from a set of triaxial tests. It will be seen from Figure 4.11 that, for an actual set of experimental results, the  $\tau_{\max}$  versus  $\sigma_y$  plot is closely related to the  $\tau_{xy}$  versus  $\sigma_y$  relation which is assumed to be defined by the Mohr envelope. This suggests that the relation proposed in equation (4.23) and a similar relation between  $\tau_{xy}$  and  $\sigma_y$  proposed by Murrell (1966) and Hobbs (1966) are not contradictory and that the advantage of using equation (4.23) depends solely upon its practical convenience<sup>4</sup>.

In order to evaluate the constants  $A$  and  $b$  in equation (4.23) for a given material, it is convenient to rewrite the equation in the following form:

$$\log_{10} \frac{\tau_{\max} - \tau_{\max o}}{\sigma_c} = \log_{10} A + b \log_{10} \frac{\sigma_m}{\sigma_c} \quad (4.24)$$

where  $\sigma_c$  is the uniaxial compressive strength of the material.

The advantage of normalizing the experimental results by dividing each measured value by the uniaxial compressive strength of a number of tests on the same plot. This advantage is obvious in Figure 4.10 in which the results of triaxial tests on the eight

---

<sup>4</sup> An interesting application of the maximum shear stress versus mean normal stress plot has been described by the author (Hoek 1966) in connection with the analysis of rock fracture around underground excavations by means of photoelastic models

sandstones listed in Table 4.1 are plotted on the same graph. Normalizing the results has the additional advantage of minimizing the influence of testing techniques, specimen sizes and environmental conditions since these conditions are usually common to both numerator and denominator of the dimensionless ratios.

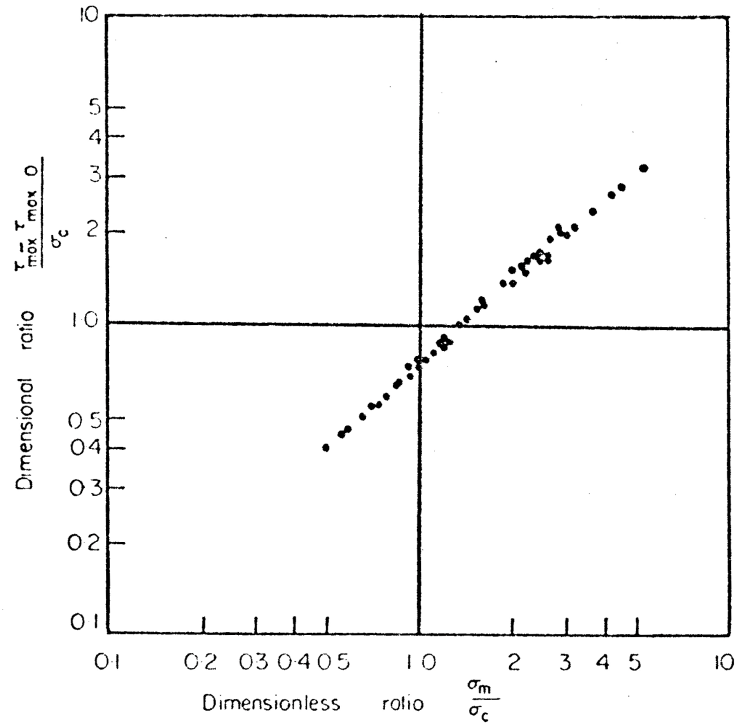


Figure 4.10 Relation between the maximum shear and mean normal stresses at rupture for sandstones

Plotting the experimental results on logarithmic scales permits a direct evaluation of the constants  $A$  and  $b$  since  $A$  is given by the value of  $(\tau_{\max} - \tau_0)/\sigma_c$  when  $\sigma_m/\sigma_c = 1$ , ( $\log_{10}(\sigma_m/\sigma_c) = 0$ ), and the value of  $b$  is given by the slope of the straight line through the experimental points. However, complete evaluation of the constants requires that the value of the intercept  $\tau_{\max 0}$  be known and, in the absence of experimental values, the author suggests that a reasonable estimate is given by  $\tau_{\max 0}/\sigma_c = 0.1$ .

Fitting the best straight line to the experimental points plotted in Figure 4.10 by the method of least squares and substitution of the resulting values of  $A$  and  $b$  into equation (4.23) gives

$$\frac{\tau_{\max}}{\sigma_c} = 0.1 + 0.76 \left( \frac{\sigma_m}{\sigma_c} \right)^{0.85} \quad (4.25)$$

which, as shown in Figure 4.11, adequately defines the rupture behaviour of the sandstones listed in Table 4.1.

Table 4.1 Sandstones included in Figure 4.10

Name	Experimenter	Country	Uniaxial compressive strength	
			lb.in <sup>2</sup>	kg/cm <sup>2</sup>
---	Jaeger	Australia	9,000	633
Darley Dale 1	Price	England	5,780	406
Pennant	Price	England	22,500	1,582
Rush Springs	Bredthauer	America	25,000	1,758
Iwaki	Horibe and Kobayashi	Japan	1,780	125
----	Everling	Germany	18,500	1,300
Darley Dale II	Murrell	England	11,500	1,300
Warmbaths	Wiid	South Africa	14,750	1,037

In Figure 4.11, a set of idealized Mohr circles and their envelope are shown and it will be noted that, having defined the relation between the maximum shear stress and mean normal stress, the construction of these circles and the fitting of the envelope is reduced to a simple and reliable graphical operation. This is in contrast to the difficulties of fitting an envelope by eye to a set of experimentally determined Mohr circles since such an envelope is invariably fitted to the circles of maximum diameter and does not take into account the scatter of the experimental values<sup>5</sup>.

<sup>5</sup> The interested reader can easily check this difficulty for himself by constructing a few Mohr circles from the experimental values given in Figure 4.11 and noting the exaggerated curvature of the envelope fitted to the maximum diameter circles.

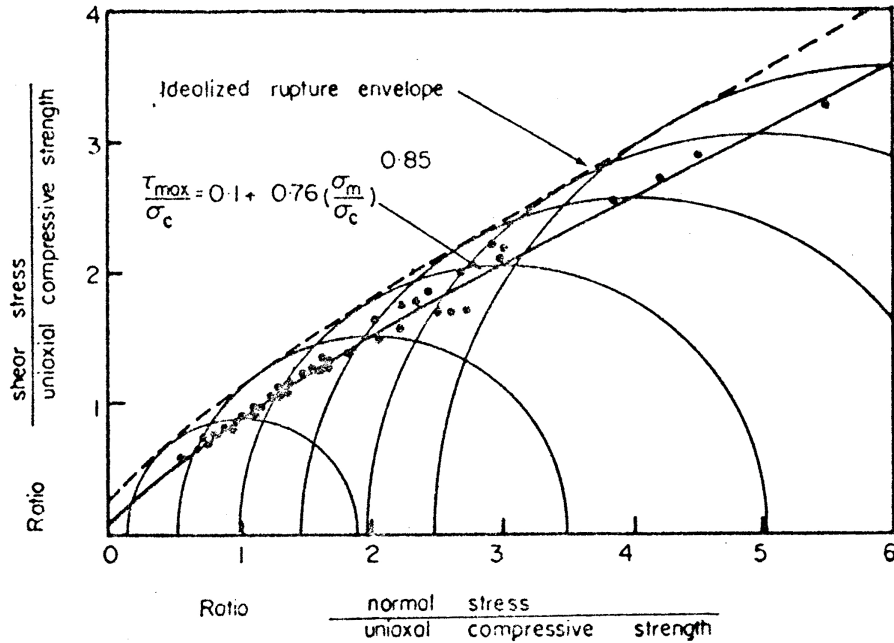


Figure 4.11 Mohr stress diagram for the rupture of sandstone.

Although no attempt is made here to develop the theoretical relation between the Mohr envelope and the  $\tau_{max}$  versus  $\sigma_y$  plot, it is interesting to examine the relation between the intrinsic shear strength  $\tau_o$  and the maximum shear stress intercept  $\tau_{max o}$ . As discussed earlier in this chapter, pure tensile rupture is assumed to occur when  $\sigma_1 \leq -3\sigma_3$  which means that all Mohr stress circles within this stress range touch the envelope at one point defined by  $\sigma_3 = \sigma_t$  (see Figure 4.8). Rupture under conditions of pure shear, i.e.  $\sigma_1 = -\sigma_3$ , falls into this category and it can be seen from Figure 4.,8 that the radius of the Mohr circle defining this condition is equal to  $\sigma_t$  and, since this circle defines the maximum shear stress intercept ( $\sigma_m = 0$ ), it follows that

$$\tau_{max o} = \pm\sigma_t \tag{4.26}$$

Comparing equations (4.20) and (4.26) gives

$$\frac{\tau_o}{\tau_{max o}} = \left( \frac{1}{\mu} + \mu \right) \tag{4.27}$$

and substitution of a range of values for  $\mu$  between 0.5 and 2 shows that a reasonable estimate for the relation between  $\tau_o$  and  $\tau_{max o}$  is given by

$$\tau_o \cong 2\tau_{\max o} \quad (4.28)$$

Although the prime purpose of plotting the triaxial test results for sandstone in Figures 4.10 and 4.11 is to demonstrate the influence of the normal stress upon the frictional behaviour of rock, these figures cannot be left without noting the remarkable similarity in the rupture behaviour of the eight sandstones which, from the information given in Table 4.1, have widely varying geographical locations and geologic materials, any attempt at an explanation of this similarity would be based on pure speculation and would be out of place in this chapter. However, since similar patterns of behaviour have been noted for many other rock types (Hoek & Bieniawski 1965; Hoek 1966), the practical significance of such patterns, even if they can only be defined by empirical relations such as that suggested by Equation (4.23), is important.

Following the thoughts which probably motivated Wuerker (1959) when he prepared his annotated tables of rock strength, it is suggested that the availability of a collection of dimensionless results, such as those presented in figure 4.10, could be of considerable assistance to the practical engineer who may have neither the time nor the facilities to carry out the large number of triaxial tests necessary to define the behaviour of the material with which he is concerned. In order to obtain an estimate of the behaviour of a particular material, it would only be necessary to determine the uniaxial compressive strength  $\sigma_c$ , under the environmental conditions and using the testing technique and size of specimen most appropriate to the particular problem under consideration. Substitution of this value of  $\sigma_c$  into the characteristic equation of that type of material (e.g. equation (4.25) for sandstone) would give a  $\tau_{\max}$  versus  $\sigma_m$  plot, and if necessary the Mohr circles and envelope, which would be sufficiently accurate for most practical purposes<sup>6</sup>. †

---

<sup>6</sup> The author wishes to make it quite clear that he does not advocate the procedure suggested above as a solution to all problems of rock testing. The curve which defines the rupture behaviour of a rock may be an extremely useful tool but it cannot replace the 'feel' of his material which an engineer can only obtain by working with it and observing its behaviour under test conditions. However, since the ever-increasing demands of progress restrict the time which the modern engineer can afford to spend on the luxury of getting to know his material, the suggested procedure, while academically unattractive to the physicist, may still prove very practical in engineering application. In order to implement the ideas outlined above, a research project has been initiated at Imperial College, London, which involves the collection and computer analysis of all available results for triaxial rock tests, using published data and whatever raw data it proves practical to obtain.

#### 4.6.2 Influence of anisotropy on the strength of rock

The ideal brittle rock, upon which most of the discussion presented thus far has been based, is assumed to contain a large number of randomly oriented flaws of equal size. These conditions would very seldom be found in practical rock mechanics problems and, hence, it is necessary to make an estimate of the probable influence of anisotropy would exceed the scope of this chapter and it will suffice to illustrate the main points of practical interest by one example.

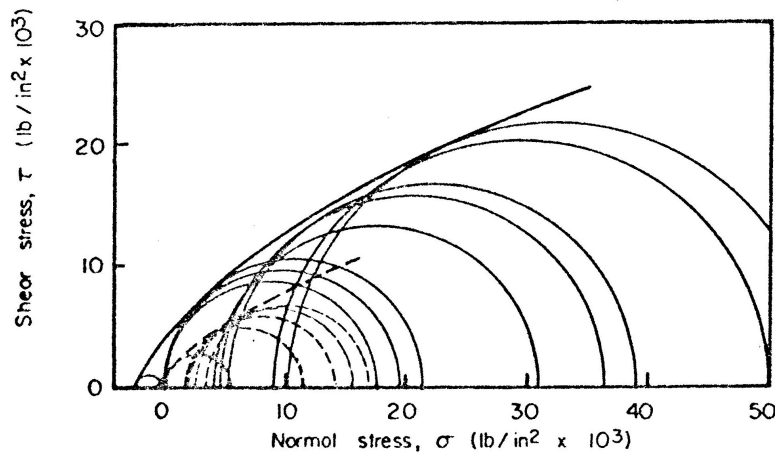


Figure 4.12 Mohr envelopes defining the rupture behaviour of the bedding planes (dashed line) and parent material (solid line) of a South African slate.

Figure 4.12 shows the rupture behaviour of a South African slate (Hoek 1964). The solid line is for tests carried out on specimens in which the bedding planes were oriented in such a way as to minimize their influence ( $\beta = 90^\circ$  for tensile tests and  $\beta = 90^\circ$  or  $0^\circ$  for compressive tests). The dashed envelope represents the results obtained from specimens in which the bedding planes were oriented to exert their maximum influence  $\beta = 0$  for tensile tests and  $\beta = \frac{1}{2} \arctan \frac{1}{\mu}$  for compression tests).

It is evident from this figure that the rupture envelope of the slate in its weakest state is merely a scaled down version of the rupture envelope for the strongest state. Plotting these results on dimensionless logarithmic scales as was done in figure 4.29 confirms that the constants  $A$  and  $b$  (equation 4.23) are not significantly different for these two rupture envelopes but Figure 4.10 shows that the value of the uniaxial compressive strength  $\sigma_c$

### *Brittle fracture of rock*

varies by a factor of approximately 4, depending upon the orientation of the bedding planes to the principal stress directions.

The practical significance of these findings is that, in problems in which the principal stress directions and major weakness planes in the material are known, the appropriate value of  $\sigma_c$  can be determined and used in analysing the rupture behaviour of the rock. Hence, for example, the analysis of the stability of a slope in which the rock contains well-defined planes of weakness must take the orientation of these planes into account. Note that, in such cases, the weakness planes may contain soft filling material which may reduce the frictional resistance of this plane, i.e. the values of  $A$  and  $b$  will differ from those of the parent material and must be determined independently.

In cases in which the orientations of the weakness planes in relation to the principal stress directions are not known, it can only be assumed that the rupture behaviour of the material will lie somewhere between the two envelopes representing its weakest and strongest states (e.g. Figure 4.12 for slate). Since this would be the case in many practical rock mechanics problems, it is suggested that, where the stability of a structure is at stake, the only safe course to follow is to use the envelope defining the weakest state of the material.

#### ***4.6.4 Influence of laboratory testing techniques upon the rupture of rock***

A large proportion of the research effort which has gone into building up the science of rock mechanics has been devoted to the detailed study of laboratory testing techniques. Jaeger (1966) has given an excellent review of this work which includes studies of the influence of specimen geometry, platen friction, rate of loading, size of specimen and of the stiffness of the testing machine upon the behaviour of the rock specimen. No useful purpose would be served by attempting to repeat the details of this review and the following discussion will be confined to certain basic principles of rock testing.

The results of presented in Figures 4.10 and 4.11 suggest that the *shape* of the characteristic curve which defines the rupture behaviour of a rock is largely independent of the method of testing. Consequently, in choosing a testing technique, which determines the *position* of the characteristic curve on the  $\tau - \sigma$  plane, it is necessary to consider:

### *Brittle fracture of rock*

a) the basic principles of materials testing which have to be fulfilled and

b) the purpose for which the test results are required.

The most important requirement which must be met in carrying out a test is that it must be possible to determine the stresses acting on the specimen. Since most rocks exhibit some degree of anisotropy and all rock become anisotropic as a point of rupture is approached (Walsh 1965; Brace, Pauling & Scholz 1966), any test specimen in which there are significant stress gradients and for which the stress at rupture has to be calculated on the basis of the theory of elasticity must be treated with suspicion. This applies to specimens tested in bending, torsion and to certain indirect tests which involve high stress gradients, e.g. indentation of the specimen with a steel ball or diamond point. The simplest solution to the problem is to choose a specimen geometry which permits calculation of the applied stresses from a simple load/area relation. However, even when this condition is met, e.g. in the case of a cylindrical specimen subjected to direct compressive stress, it is still necessary to ensure that stress gradients are not induced as a result of poor end conditions (Hoek 1966, Mogi, 1966).

The purpose for which the results of laboratory tests on rock specimens is required can have an important bearing upon the test method chosen. This is particularly true in relation to the direction of the most important failure surface in a ruptured specimen (Figure 4.7). For example, if the results of a set of laboratory tests are to be applied to a slope stability problem in which the shear rupture mode (Figure 4.7a) is of prime importance, an applied stress condition which encourages the development of this shear mode, i.e. a shear-box test, would be a logical choice for the test method.

In the case of the rock surrounding underground mine excavations, both tensile and shear modes may be important. An even more important consideration may be the stress redistribution associated with fracture which may result in the load on an element being relieved if it tends to deform by a large amount in relation to the surrounding rock. An appreciation of this problem has led to the development of 'stiff-machine' testing techniques (Cook and Hojem 1966; Bieniawski in submission) which restrict the strain which takes place in the specimen.

The conclusion to be drawn from the discussion presented above is that, while it is

important to exercise care in preparing and testing rock specimens, it is even more important to give serious consideration to the use to which the results are to be put. Unless the test method chosen bears a direct relation to the problem under consideration, a great deal of effort can be expended on obtaining information which may have little or no practical significance.

## **References**

- Bieniawski, Z.T. Paper submitted. Mechanism of brittle fracture of rock. submitted to *Intern. J. Rock Mech. Mining Sci.*
- Brace, W.F. and E.G. Bombolakis 1963. A note on brittle crack growth in compression, *J. Geophys. Res.*, 68, No. 12, 3709-3713.
- Brace, W.F., Paulding, B.W. and C. Scholz 1966. Dilatancy and fracture of crystalline rocks, *J. Geophys. Res.*, 71, No. 16, 3939-3953.
- Bray, J.W. personal communication.
- Byerlee, J.D. In press. A theory of friction based on brittle fracture, *J. Appl Phys.*
- Byerlee, J.D. In press. The frictional characteristics of granite under high confining pressure, *J. Geophys. Res.*
- Colback, P.S.B. and B. L. Wiid 1965 The influence of moisture content on the compressive strength of rock, *Proc. Symp. Rock Mech.*, 3rd, Toronto.
- Cook, N.G.W. and J.P.M. Hojem, 1966. A rigid 50-ton compression and tension testing machine. *S. African Mech. Engr.*, Nov., 89-92.
- Denkhaus, H.G. 1964. The application of the mathematical theory of elasticity to problems of stress in hard rock at great depth. *Bull. Inst. Mining Met.*, 68, 283-309.
- Donath, F.A. 1964. Strength variation and deformation behaviour in anisotropic rock. In *State of Stress in the Earth's Crust* (Ed. W.R. Judd), Elsevier: New York, pp. 281-298.
- Griffith, A.A. 1924. Theory of rupture, *Intern. Congr. Appl. Mech.*, 1st, Delft, 55-63.
- Griffith, A.A. 1921. The phenomena of rupture and flow in solids. *Phil. Trans. Roy. Soc. London, Series A*, 221, 163-198.
- Hobbs, D.W. 1966. A study of the behaviour of broken rock under triaxial compression,

*Brittle fracture of rock*

- and its application to mine roadways, *Intern. J. Rock Mech. Mining Sci.*, 3, 11-43.
- Hoek, E. 1964. Fracture of anisotropic rock. *J. S. African Inst. Mining Met.*, 64, 510-518.
- Hoek, E. 1966. A photoelastic technique for the determination of potential fracture zones in rock structures. *Symp. Rock Mech.*, Minnesota, (Proceedings to be published by AIME, 1967).
- Hoek, E. 1966. Rock mechanics - an introduction for the practical engineer. *Mining Mag.* (London), April, June, July issues.
- Hoek, E. and Z. T. Bieniawski 1965. Brittle fracture propagation in rock under compression, *Intern. J. Fracture Mech.*, 1, No. 3, 137-155.
- Inglis, C.E. 1913. Stresses in a plate due to the presence of cracks and sharp corners, *Trans. Inst. Naval Architects*, London, 55, Part I, 219-230.
- Jaeger, J.C. 1966. The brittle fracture of rocks. *Symp. Rock Mech.*, Minnesota, (Proceedings to be published by AIME, 1967).
- K. Mogi 1966. Some precise measurements of fracture strength of rocks under uniform compressive stress, *Rock Mech. Eng. Geol.*, 4, Part 1, 43-55.
- Murrell, S.A.F. 1966. The effect of triaxial stress systems on the strength of rocks at atmospheric temperatures, *Geophys. J.*, 10, No. 3, 231-281.
- Patton, F.D. 1966. Multiple modes of shear failure in rock, *Proc. Intern. Congr. Rock Mech.*, Lisbon, 509-514.
- Paul, B. and M. Gangal 1966. Initial and subsequent fracture curves for biaxial compression of brittle materials, *Symp. Rock Mech.*, Minnesota, 1966 (Proceedings to be published by AIME, 1967).
- Walsh, J. B. and W. F. Brace 1964. A fracture criterion for anisotropic rock. *Geophys. Res.*, 69, No. 16, 3449-3456.
- Walsh, J.B. 1965. The effect of cracks on the compressibility of rock, *Geophys. Res.*, 70, No. 2, 381-389.
- Wuerker, R.D. 1959. Annotated tables of strength of rock, *Trans. AIME (Petrol. Div)*, No. 663-669.